The Role of Hydrogen Bonds for the Multiphasic $P680^{+\bullet}$ Reduction by Y_Z in Photosystem II with Intact Oxyen Evolution Capacity. Analysis of Kinetic H/D Isotope Exchange Effects[†]

G. Christen and G. Renger*

Max-Volmer-Institute for Biophysical Chemistry and Biochemistry, Technical University Berlin, Strasse des 17. Juni 135, 10623 Berlin, Germany

Received September 10, 1998; Revised Manuscript Received October 29, 1998

ABSTRACT: The mechanism of multiphasic $P680^{+\bullet}$ reduction by Y_Z has been analyzed by studying H/D isotope exchange effects on flash-induced changes of 830 nm absorption, $\Delta A_{830}(t)$, and normalized fluorescence yield, $F(t)/F_0$, in dark-adapted thylakoids and PS II membrane fragments from spinach. It was found that (a) the characteristic period four oscillations of the normalized components of $\Delta A_{830}(t)$ relaxation and of $F(t)/F_0$ rise in the nanosecond and microsecond time domain are significantly modified when exchangeable protons are replaced by deuterons; (b) in marked contrast to the normalized steady-state extent of the microsecond kinetics of 830 nm absorption changes which increases only slightly due to H/D exchange (about 10%) the S_i state-dependent pattern exhibits marked effects that are most pronounced after the first, fourth, fifth, and eighth flashes; (c) regardless of data evaluation by different fit procedures the results lead to a consistent conclusion, that is, the relative extent of the back reaction between $P680^{+\bullet}Q_A^{-\bullet}$ becomes enhanced in samples suspended in D_2O; and (d) this enhancement is dependent on the S_i state of the WOC and attains maximum values in S_2 and S_3, most likely due to a retardation of the "35 μs kinetics" of $P680^{+\bullet}$ reduction. In an extension of our previous suggestion on the functional role of hydrogen bonding of Y_Z by a basic group X (Eckert, H.-J., and Renger, G. (1988) *FEBS Lett. 236*, 425−431), a model is proposed for the origin of the multiphasic $P680^{+\bullet}$ reduction by Y_Z. Two types of different processes are involved: (a) electron transfer in the nanosecond time domain is determined by strength and geometry of the hydrogen bond between the O−H group of Y_Z and acceptor X, and (b) the microsecond kinetics reflect relaxation processes of a hydrogen bond network giving rise to a shift of the equilibrium $P680^{+\bullet}Y_Z \rightleftharpoons P680Y_Z^{OX}$ toward the right side. The implications of this model are discussed.

Photosynthetic water oxidation to molecular oxygen and four protons takes place via a sequence of redox steps at a manganese-containing operational unit referred to as water-oxidizing complex (WOC)[1] (for reviews, see refs *1*−*3*). This process is energetically driven by the chlorophyll cation radical $P680^{+\bullet}$ that is formed as a result of the primary charge separation in Photosystem II (PS II) (for review, see ref *4*). The strongly oxidizing species $P680^{+\bullet}$ extracts stepwise electrons from the WOC with tyrosine residue 161 (Y_Z) of polypeptide D1 (*5*, *6*) acting as intermediary redox carrier. The oxidized form Y_Z^{OX} appears to be in EPR studies as a neutral radical (*7*) with the proton from the phenolic group being either localized at a nearby base X as proposed in (*8*) or released into the lumen (*9*). As a consequence of these two alternatives Y_Z^{OX} is discussed to act either as redox carrier in a conventional manner of electron transfer or as specific hydrogen abstractor from substrate (H_2O or OH^-) coordinated to manganese (for further discussion, see refs *10*, *11*). The kinetics of both $P680^{+\bullet}$ reduction by Y_Z and stepwise WOC oxidation by Y_Z^{OX} depend on the redox state S_i of the WOC (for a compilation of data, see ref *12*). The former reaction is dominated by nanosecond kinetics (*8*, *13*−*15*).

In addition a smaller PS II fraction exhibits a $P680^{+\bullet}$ reduction with at least three components of about 3, 35, and 150 μs. The normalized extent of the microsecond kinetics is about 30% at room temperature. Consensus exists that the nanosecond kinetics are characteristic for PS II complexes with a basically intact WOC that can be modified only slightly by specific types of substances without eliminating this fast $P680^{+\bullet}$ reduction (*16*). After destruction of the WOC by treatments such as Tris washing (*17*), incubation with NH_2OH at high concentration (*18*), or trypsin treatment in the alkaline (*20*) the ns kinetics of $P680^{+\bullet}$-reduction by Y_Z disappear and are replaced by kinetics which exhibit a striking pH dependence (*19*−*21*).

In these samples the electron transfer from Y_Z to $P680^{+\bullet}$ is dominated by a 10 μs component at pH = 6.5 (*19*−*21*).

[†] The financial support by Deutsche Forschungsgemeinschaft (Re 354/10-3 and Re 354/17-4) is gratefully acknowledged.

* Corresponding author.

[1] Abbreviations: ^{3}Car, carotenoid triplet; Chl, chlorophyll; DCBQ, 2,6-dichloro-*p*-benzoquinone; fwhm, full width at half-maximum; LHCII, light harvesting complex II, MES, morpholinoethane sulfonic acid; P680, photoactive chlorophyll of PS II; PS II, photosystem II; WOC, water-oxidizing complex; Y_Z, redox active tyrosine between WOC and P680.

10.1021/bi982188t CCC: $18.00
Published on Web 01/30/1999

These kinetics and their characteristic pH dependence are a general feature that is observed when the PS II complex is deprived of an intact WOC in thylakoids (*19*), inside-out vesicles (*20*), and PS II membrane fragments (*21*). It originates from a marked increase of the activation energy from about 10 kJ/mol in systems with intact WOC (*8*) to 30−40 kJ/mol in systems lacking a functionally competent WOC (*22*−*24*). A recent analysis within the framework of the Marcus theory revealed that the reorganization energy of this reaction increases from 0.5 to 1.6 eV due to destruction of the WOC. This effect was ascribed to a drastic increase of the number of water molecules in the neighborhood of Y_Z (*24*) in line with previous conclusions drawn on the basis of EPR studies (*9*). In the oxidized form Y_Z^{OX} is unable to act as donor and $P680^{+\bullet}$ becomes reduced by $Q_A^{-\bullet}$ via a 130−200 μs kinetics (*25*−*27*). On the basis of the above-mentioned findings, all microsecond kinetics of $P680^{+\bullet}$ reduction were assumed to originate from PS II complexes that are lacking an intact WOC (*28*, *29*). However, this idea is difficult to reconcile with the period four oscillation of the amplitudes of most microsecond components when dark-adapted samples are excited with a train of saturating laser flashes. If this characteristic feature is used as a fingerprint for an intact WOC, the pronounced oscillation patterns observed for both the "3 and 35 μs kinetics" (*29*−*33*) strongly support the idea that they reflect $P680^+$ reduction by Y_Z in PS II complexes containing the WOC (*30*, *32*−*34*) while the lacking (or at most very weak) oscillation of the 150 μs kinetics is probably indicative for PS II centers without an intact WOC (*33*). The nature of the reactions leading to the "3 μs kinetics" and "35 μs kinetics" is not yet clarified. It was proposed that the "35 μs kinetics" reflect a recombination reaction (*35*), the reduction by carotenoids (*36*), or the reduction of a $Chl^{+\bullet}$ molecule different from $P680^{+\bullet}$ (*37*). Recently it was ascribed to a stabilizing relaxation process. In this case the period four oscillation of the amplitudes was explained by a S_i state-dependent redox equilibrium between $P680^{+\bullet}/Y_Z$ and $P680/Y_Z^{ox}$, but the seemingly independent 20−40 μs kinetics are difficult to reconcile with this idea (*32*, *33*).

As an attempt to gather more information a comparative study was performed that comprises measurements of flash-induced changes of the 830 nm absorption and of the relative fluorescence quantum yield in the microsecond time domain. On the basis of the results obtained it was inferred that the "35 μs kinetics" reflect a more complex reaction of at least two processes: (i) $P680^+$ reduction by Y_Z, and (ii) coupling and/or competing reaction(s) which give rise to additional increase of the Chl fluorescence yield (*33*).

Further insight into the underlying mechanism(s) can be obtained by analyzing kinetic isotope exchange effects on the rate of P680 reduction because it was recently shown that the nanosecond kinetics remain almost unaffected (*38*) whereas the "10 μs kinetics" (at pH = 6.5) in samples deprived of the WOC exhibit a pronounced retardation by a factor of about 3 when H_2O is replaced by D_2O (*23*, *24*, *38*−*40*). Latest measurements of flash-induced 830 nm absorption changes indicate that also in samples with an intact WOC the microsecond kinetics of $P680^{+\bullet}$ reduction are prone to a marked H/D exchange effect that depends on the redox state S_i of the WOC. On the basis of these data, the slower processes of $P680^{+\bullet}$ reduction were inferred to involve S_i state-dependent intraprotein proton/hydrogen transfer (*32*). Unfortunately, the time window of these measurements was restricted to 45 μs, and therefore, the information on the microsecond kinetics is limited. Furthermore, the samples contained a significant amount of Triton X-100 that might affect the mode of the presumed proton movement. As an attempt to analyze the mechanism of $P680^{+\bullet}$ by Y_Z we performed comparative studies in the microsecond time domain for both the relaxation kinetics of flash-induced 830 nm absorption changes and the rise of flash-induced relative fluorescence quantum yield. The data reported in this study reveal that a marked H/D isotope exchange effect arises for the $P680^{+\bullet}$ reduction pattern as a function of the redox state S_i of the WOC, most likely due to a S_i state-dependent retardation of the "35 μs kinetics".

MATERIALS AND METHODS

Thylakoid membranes were isolated from spinach as described in ref *41*. PS II membrane fragments were prepared from spinach as described by Berthold et al. (*42*) with slight modifications according to Völker et al. (*43*). For H/D-exchange experiments, concentrated PS II samples at a chlorophyll content of 4−8 mg/mL were suspended in a large excess of D_2O (99.9% D, Euriso-top) buffer solution.

Flash-induced changes of the fluorescence quantum qield with a time resolution of about 500 ns were monitored with home-built equipment (*33*, *44*). Fluorescence measurements were performed with spinach thylakoids ([Chl] = 20 μg/mL) in the absence of artificial acceptors at 4 °C.

Flash-induced absorption changes at 830 nm with a microsecond time resolution (maximum electrical bandwidth: 300 kHz) were measured with a single beam flash photometer as outlined previously (*16*, *33*). The absorption measurements were performed with PS II membrane fragments at a concentration of 70 μg of Chl/mL at 4 °C.

The buffer medium contained 10 mM NaCl and 50 mM buffer (succinic acid (pL 4.0−5.0), MES (pL 5.5−6.5), and HEPES (pL 7.0−8.0)). The addition of artificial electron acceptors is indicated in the figure captions. The pL (L = H or D) values of the buffer solutions were adjusted using a glass electrode with corrections according to Glasoe et al. (*45*).

The samples were excited by 10 ns (fwhm) laser flashes at 532 nm from a frequency-doubled Nd:YAG laser at a repetition rate of 1 Hz. Absorption changes were fitted with three exponentials and a constant using a Levenberg-Marquart fitting procedure.

Time-resolved fluorescence yield changes were fitted with a special evolution strategy fit according to Ostermeier (*46*) taking into account the nonlinear relationship between fluorescence quantum yield and quencher concentration due to the connectivity of PS II units by excitation energy transfer (*47*). Values of $a = 0.7$ and $p = 0.5$ were used for the fraction of connected centers and transfer probability, respectively (*48*).

RESULTS

Flash-Induced Absorption Changes at 830 nm. Figure 1 shows transient 830 nm absorption changes that are induced by a train of eight saturating laser flashes in dark-adapted

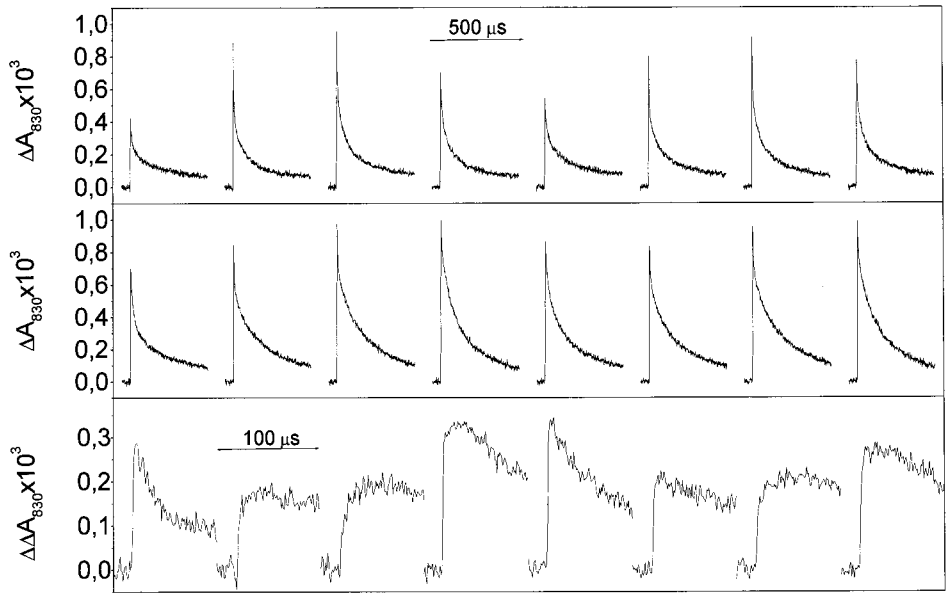

FIGURE 1: Absorption changes at 830 nm induced by a train of eight saturating laser flashes (dark time 1 s) at 4 °C in dark-adapted PS II membrane fragments from spinach suspended in either H_2O-, (top panel) or D_2O- (middle panel) containing buffer at pH(pD) = 6.5: electron acceptor, 200 μM DCBQ; sweep time, 500 μs. The signals shown represent the average of 30 traces which were each induced by the train of 8 flashes. Other experimental conditions as were described in Materials and Methods. Bottom panel: difference between the traces of top and middle panels.

PS II membrane fragments suspended either in H_2O- (top traces) or D_2O- (middle traces) containing buffer (these samples will be referred to as "H_2O sample" and "D_2O sample", respectively, throughout the paper) at 4 °C (the experimental uncertainty of these measurements is generally about 10%). At first glance these data reveal two striking features: (i) the pronounced period four oscillation pattern of the detectable initial amplitudes, observed in the H_2O sample with maxima after the third and seventh flashes and minima after the first and fifth flashes, almost fades out in the D_2O sample, and (ii) the detectable relaxation kinetics of the 830 nm absorption changes slowed when samples were suspended in D_2O- instead of H_2O-containing buffer. To illustrate the effects caused by H/D exchange, we calculated the difference between the top and middle traces, and they are depicted in the bottom part of Figure 1. For the sake of direct comparison with fluorescence data the time scale for these difference signals is enlarged (100 μs sweep). The bottom traces clearly indicate that both amplitude and kinetics are markedly affected.

A more detailed analysis of these phenomena requires suitable data evaluation to extract effects on the amplitudes and kinetics of each decay component. Since most of the relaxation in the nanosecond time range escapes the detection due to limited time resolution, the maximum initial amplitudes were determined by measurements with NH_2OH-treated samples and the data normalized to these $\Delta A_{830,max}$ values as outlined in ref *33*.

At first a target fit was performed with three exponential decay components where the half-lifetimes were kept constant at 3, 35, and 150 μs. In addition a small constant offset was used to account for contributions that are very slow compared with the sweep time. The results obtained are summarized in Figure 2 and Table 1.

In the H_2O sample the 3 and 35 μs kinetics exhibit pronounced oscillations whereas the 150 μs kinetics and the offset are almost independent of the flash number. These

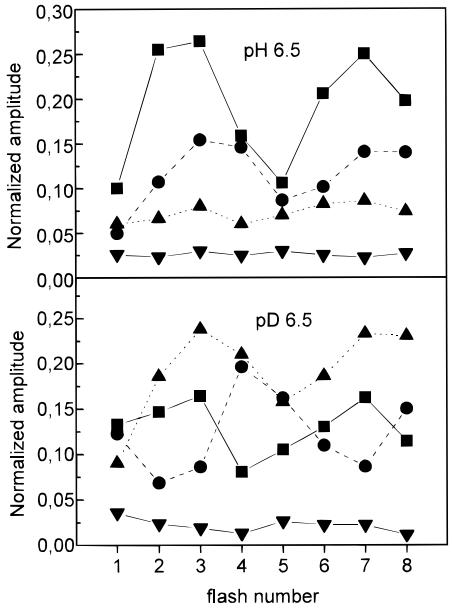

FIGURE 2: Normalized amplitudes of the decay components of $\Delta A_{830}(t)$ with fixed half-lifetimes of 3 μs (squares), 35 μs (circles), and 150 μs (triangles) and offset (inversed triangles) as a function of flash number in PS II membrane fragments suspended in H_2O- (top panel) and D_2O- (bottom panel) containing buffer. The data were obtained by a target fit with fixed half-lifetimes of the traces shown in Figure 1 (see text).

findings are in close correspondence with previous reports (*8*, *14*, *31*, *33*). A markedly different pattern is observed for the D_2O sample. The most surprising result is the apparent period four oscillation of the amplitude of the 150 μs kinetics that is typical for the back reaction between $P680^{+\bullet}$ and $Q_A^{-\bullet}$ when Y_Z^{OX} is present (*25*−*27*). Accordingly, in the H_2O sample these kinetics are ascribed to a small fraction of PS II with Y_Z^{OX} kept oxidized between the flashes. As the amplitudes of the 150 μs kinetics do not exhibit a marked period four oscillation, it seems likely that they originate to

Table 1: Target Fit of the Data of Figure 1 with Fixed Half-Lifetimes of 3, 35, and 150 μs[a]

flash number	$A_{3\mu s}$	$A_{35\mu s}$	$A_{150\mu s}$	A_{ss}	ζ^2
		Target Fit pH 6.5			
1	0.10	0.05	0.06	0.03	1.48
2	0.25	0.11	0.07	0.02	1.64
3	0.26	0.15	0.08	0.03	1.20
4	0.16	0.15	0.06	0.02	1.60
5	0.11	0.09	0.07	0.03	1.52
6	0.21	0.10	0.08	0.02	1.29
7	0.25	0.14	0.09	0.02	1.32
8	0.20	0.14	0.07	0.03	1.46
		Target Fit pD 6.5			
1	0.13	0.12	0.09	0.04	2.95
2	0.15	0.07	0.19	0.02	1.28
3	0.16	0.09	0.24	0.02	1.44
4	0.08	0.20	0.21	0.01	1.42
5	0.10	0.16	0.16	0.03	2.07
6	0.13	0.11	0.19	0.02	1.32
7	0.16	0.09	0.23	0.02	1.32
8	0.11	0.15	0.23	0.01	1.71

[a] $\Delta A_{830}(t) = A_{3\mu s} \exp(-t/4.33) + A_{35\mu s} \exp(-t/50.5) + A_{150\mu s} \exp(-t/215) + A_{ss}$.

a large extent if not completely from complexes that are lacking an intact WOC. Measurements of the oxygen evolution capacity prove that replacement of exchangeable protons by deuterons does not affect the functional integrity of the WOC (*38*) but rather increases its thermal stability (*49*, *50*). Therefore, the significant enhancement and the oscillation of the amplitudes of the 150 μs kinetics in the D_2O sample cannot be ascribed to a decrease of the PS II fraction with an intact WOC. In principle, two different mechanisms can be offered as explanation: (i) increased and S_i state-dependent population of Y_Z^{OX} or (ii) marked retardation of the 35 μs kinetics by an H/D isotope exchange effect analogous to that observed for P680$^{+\bullet}$ reduction by Y_Z in samples lacking a functionally competent WOC (*23*, *24*, *40*). In an attempt to gather further information which permits a distinction between these alternatives, we compared the oscillation pattern of the difference of the values $\Delta A_{n,150\mu s}(D_2O) - \Delta A_{n,150\mu s}(H_2O)$ (calculated from the data of Table 1) with that of the normalized amplitudes of the 35 μs kinetics in the H_2O sample. Both parameters exhibit a very similar period four oscillation. This finding supports the idea that the 35 μs kinetics are prone to a marked kinetic H/D isotope effect. Therefore the second type of mechanism has been analyzed in more detail by performing another type of target fit. In this case the amplitudes of the 150 μs kinetics observed in D_2O samples are assumed to be a composite of two contributions, that is, a constant fraction due to P680$^{+\bullet}$Q$_A^{-\bullet}$ recombination (vide supra) and an oscillating retarded 35 μs kinetics. To extract the extent of the latter contribution, we subtracted a constant fraction of the 150 μs kinetics from the detected signals of both sample types because P680$^{+\bullet}$ reduction by Q$_A^{-\bullet}$ was recently found to lack a kinetic H/D isotope exchange effect (*40*). The extent of this constant fraction was assumed to correspond with amplitudes of the 150 μs kinetics after the first flash where they attain minimum values of 0.06 (H_2O sample) and 0.09 (D_2O sample). After subtraction of these constant fractions from all signals of the sequence, the remaining transients were subjected to a fit procedure where the other parameters were free running. The results obtained are shown in Figure 3 and compiled in Table 2. At a first glance, the oscillation pattern of the normalized amplitudes of the fast (3 μs kinetics) and the middle (35 μs kinetics) decay components is not markedly changed in the H_2O sample compared with that gathered from the target fit with fixed half-lifetimes (see Figure 2). However, a closer inspection of the data readily shows that the half-lifetimes of the fast kinetics exhibit a characteristic period four oscillation with minimum values of 2−3.5 μs after the second, third, sixth, and seventh flashes and maximum values of 5−7 μs after flashes no. 1, 4, 5, and 8. An analogous feature emerges for the D_2O sample, but in this case the effect is more pronounced. In fact, the fast kinetics appear to be a composite of two components with S_i state-dependent amplitudes, and the slower one (5−7 μs) seems more affected by H/D exchange. These details, however, will not be further analyzed in this study. In marked

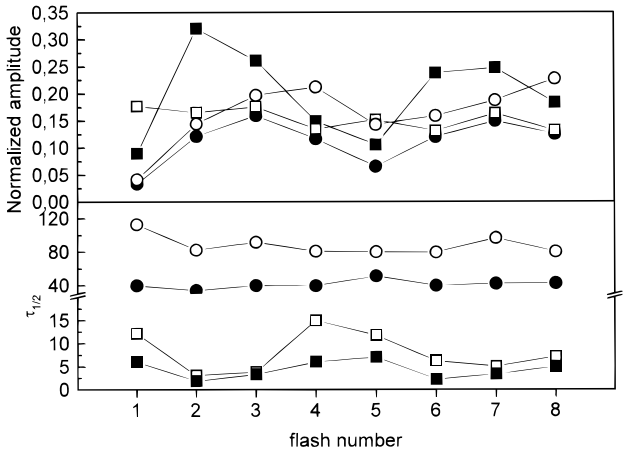

FIGURE 3: Normalized amplitudes (top panel) and half-lifetimes (bottom panel) of fast (squares) and middle (circles) decay components $\Delta A_{830}(t)$ as a function of flash number in PS II membrane fragments suspended in H_2O- (filled symbols) or D_2O- (open symbols) containing buffer. The data were obtained by a target fit with a constant fraction of the 150 μs component (fixed half-lifetime) and free running parameters for amplitudes and half-lifetimes for the fast and middle decay component (see text).

Table 2: Target of the Data of Figure 1 with Fixed 150 μs Kinetics (Constant Amplitude) and Fast and Middle Component as Free Running Parameter (Amplitude and Half-Lifetime)

flash number	A_f	$\tau_{1/2,f}$	A_m	$\tau_{1/2,m}$	A_{ss}	ζ^2
			H_2O Sample[a]			
1	0.09	6.0	0.03	40	0.03	1.35
2	0.32	1.9	0.12	34	0.02	1.27
3	0.26	3.3	0.16	40	0.03	1.31
4	0.15	6.0	0.12	40	0.02	1.28
5	0.11	7.1	0.07	51	0.03	1.33
6	0.24	2.3	0.12	40	0.03	1.28
7	0.25	3.3	0.15	42	0.03	1.52
8	0.18	5.0	0.13	43	0.03	1.54
			D_2O Sample[b]			
1	0.18	12	0.04	113	0.03	1.37
2	0.16	3.2	0.14	82	0.03	1.50
3	0.18	3.9	0.20	92	0.03	1.73
4	0.13	15	0.21	81	0.03	1.80
5	0.15	12	0.14	80	0.03	1.55
6	0.13	6.2	0.16	80	0.03	1.43
7	0.16	5.1	0.19	97	0.03	1.58
8	0.13	7.2	0.23	80	0.03	2.00

[a] $\Delta A_{830}(t) = A_f \exp(-(t/\tau_f)) + A_m \exp(-t/\tau_m)) + 0.06 \exp(-(t/215)) + A_{ss}$. [b] $\Delta A_{830}(t) = A_f \exp(-(t/\tau_f)) + A_m \exp(-t/\tau_m)) + 0.09 \exp(-(t/215)) + A_{ss}$.

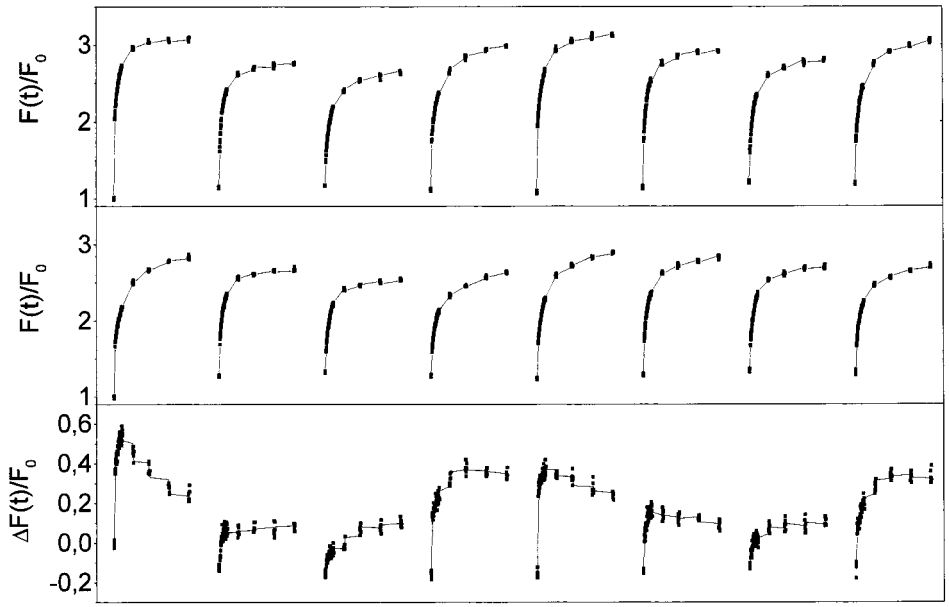

FIGURE 4: Normalized changes of the fluorescence quantum yield $F(t)/F_0$ induced by a train of saturating laser flashes (dark time 1 s) at 4 °C in dark-adapted spinach thylakoids suspended in either H_2O- (top panel) or D_2O- (middle panel) containing buffer at pH(pD) = 6.5 in the absence of exogenous electron acceptors. The signals shown represent the average of two different thylakoid preparations and of 8 traces induced by the flash train in each sample: sweep time, 100 μs. Other experimental conditions were as described in Materials and Methods. Bottom panel: difference between the traces of top and middle panels.

contrast the half-lifetimes of the middle components remain invariant within a rather narrow span of ±20% compared with the average values of about 40 and about 85 μs in H_2O sample and D_2O sample, respectively.

Regardless of the differences between these two fit procedures, both of them lead to virtually the same conclusion with respect to the average values of the microsecond component: the normalized extent of all microsecond components averaged over the eight flashes results for both methods to the same values of 0.41 ± 0.02 for the H_2O sample and 0.45 ± 0.03 for the D_2O sample. This finding indicates that the extent of these averaged amplitudes is almost independent of the replacement of exchangeable protons by deuterons, in perfect agreement with recent measurements performed with PS II core complexes at high time resolutions and excellent signal/noise ratios (*38*). This study convincingly showed that, under repetitive laser flash excitation $P680^{+\bullet}$ reduction in the ns time domain neither exhibits any significant kinetic H/D isotope exchange effect ($\leq$1.05) nor exhibits a change of the normalized extent of these kinetics (*38*). It has to be emphasized that the experiments of the present study were performed at 4 °C, and therefore, the average extent of the microsecond kinetics is larger (about 40%) than that of about 30% determined at room temperature (*38*). This temperature effect will not be analyzed in the present study.

In marked contrast to the steady-state properties, a completely different feature emerges when taking into account the dependence of $P680^{+\bullet}$ reduction kinetics on the redox state S_i of the WOC. As a result of the analyses performed so far in the present study, it is clear that the $P680^{+\bullet}$ reduction in the microsecond time domain exhibits a marked H/D isotope exchange effect. Depending on the mode of data fit, the dominant effect is either a marked increase of the population of Y_Z^{OX} that depends on the redox state S_i of the WOC (Figure 2, Table 1) or a S_i state-dependent retardation of the kinetics of both the fast (3 μs) and the middle (35 μs) phase by a factor of 2−3 (Figure 3, Table 2). The above-mentioned considerations support the latter mechanism. The general finding of an S_i state-dependent H/D exchange effect is in nice agreement with a recent report of Schilstra et al. (*32*), but differences exist with respect to the details of this feature, probably originating from the limited time window of 45 μs that was used in ref *32*. Furthermore, data interpretation is largely extended by comparative fluorescence measurement, especially with respect to the competition with $P680^{+\bullet}Q_A^{-\bullet}$ recombination (vide infra).

Flash-Induced Changes of the Relative Fluorescence Quantum Yield. To obtain complementary information, we performed comparative measurements for the flash-induced rise of the relative fluorescence quantum yield that reflects $P680^{+\bullet}$ reduction (*51*). The measurements were performed with a time resolution of 500 ns and a sweep time of about 100 μs as outlined in refs *33* and *44*. The results obtained by excitation with a train of eight saturating laser flashes in the H_2O sample and D_2O sample of spinach thylakoids are shown in the top and middle parts, respectively, of Figure 4. The traces of both patterns exhibit a characteristic period four oscillation. They also reveal marked differences originating from H_2O/D_2O exchange. For better illustration, the differences of the signals were determined and depicted in the bottom part of Figure 4. Basically the same features emerge as those observed for the 830 nm absorption changes [for comparison, see Figure 1, bottom traces at the same time scale], that is, comparatively large effects after the first, fourth, fifth, and eighth flashes and markedly less pronounced changes after flashes no. 2, 3, 6, and 7. This finding indicates that both techniques monitor essentially the same H/D exchange effects on $P680^{+\bullet}$ reduction.

Apart from the correction for the nonlinear relationship between quencher concentration and fluorescence yield (see

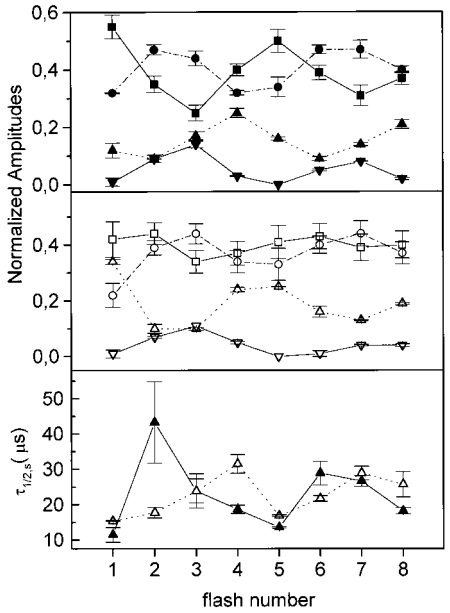

FIGURE 5: Normalized amplitudes of the rise components of $F(t)/F_0$ with fixed half-lifetimes of 200 ns (squares) and 3 μs (circles), middle component with half-lifetime as free running parameter (triangles), and offset (inverse triangles) as a function of flash number in spinach thylakoids suspended in H_2O- (top panel) and D_2O- (middle panel) containing buffer. The bottom panel shows the dependence of the half-lifetime $\tau_{1/2}$ on the flash number in H_2O sample (filled triangles) and D_2O sample (open triangles). The data were obtained by a target fit of the traces shown in Figure 4 after correction for excitation energy transfer between different photosynthetic units (see text). The error bars indicate the spread of results over experiments with two different thylakoid preparations. Error bars were omitted when both fits led to the same result.

Materials and Methods), two additional effects have to be taken into account when P680$^{+\bullet}$ reduction is monitored through transients of the fluorescence yield: (i) the recombination reaction P680$^{+\bullet}$Q$_A^{-\bullet}$ → P680Q$_A$ cannot be detected via a flash-induced rise of the relative fluorescence quantum yield because the disappearance of the quencher P680$^{+\bullet}$ is counterbalanced by the synchronous formation of quencher Q$_A$; and (ii) interference with the decay kinetics of carotenoid triplets that act as fluorescence quenchers (vide infra).

It has to be emphasized that the first effect provides a suitable tool to distinguish P680$^{+\bullet}$ reduction by Q$_A^{-\bullet}$ from that of other donors such as Y$_Z$. This great advantage of complementary information by the fluorometric method will be illustrated later (vide infra).

In a first attempt a target fit was performed where the unresolved kinetics in the nanosecond time domain are described by a very fast component of variable amplitude and the $\tau_{1/2}$ value fixed at 200 ns. Two kinetics were used to fit the resolved rise in the microsecond time domain, that is, a fast component of fixed 3 μs half-lifetime and variable amplitude and a middle component where both amplitude and half-lifetime were free running parameters. Furthermore, an offset of variable extent was taken into account. The results obtained are depicted in Figure 5 and summarized in Table 3. It has been carefully checked that a variation of the lifetime of the nanosecond component up to a reasonable upper limit of 300 ns (a H/D exchange does not affect these kinetics, see ref 38) did not modify the pattern (data not shown). All components of the H_2O sample exhibit characteristic period four oscillations. The feature of the nanosecond component corresponds with those depicted in ref *33*. Likewise, the pattern of the offset is fully consistent with the S$_i$ state dependence of the fluorescence quantum yield of PS II. This phenomenon is well-established since the early reports of more than 25 years ago (*52*, *53*). It will not be discussed here. This phenomenon is not significantly affected by H/D exchange (see Figure 5 and Table 3).

Table 3: Target Fit with Three Exponentials and Fixed Half-Times of 200 ns and 3 μs and Variable Half-Lifetime of A_m[a]

flash number	A_{200ns}	$A_{3\mu s}$	A_m	$\tau_{1/2}$	A_{ss}
		pH 6.5			
1	0.55	0.32	0.12	11	0.01
2	0.35	0.47	0.09	43	0.09
3	0.25	0.44	0.17	24	0.14
4	0.40	0.32	0.25	19	0.03
5	0.50	0.34	0.16	14	0.00
6	0.39	0.47	0.09	29	0.05
7	0.31	0.47	0.14	27	0.08
8	0.37	0.40	0.21	18	0.02
		pD 6.5			
1	0.42	0.22	0.34	15	0.01
2	0.44	0.39	0.10	18	0.07
3	0.34	0.44	0.10	24	0.11
4	0.37	0.34	0.24	31	0.05
5	0.41	0.33	0.25	17	0.00
6	0.43	0.40	0.16	22	0.01
7	0.39	0.44	0.13	29	0.04
8	0.40	0.37	0.19	26	0.04

[a] The experimental data were corrected for the nonlinear relation between fluorescence yield and quencher concentration as described in Materials and Methods.

The interpretation of the microsecond kinetics requires a more detailed analysis. A general complication arises for the 3 μs rise of the fluorescence quantum yield because of interference with the decay of carotenoid triplets (see ref *54* and references therein) that act as efficient fluorescence quenchers (for recent discussion, see refs *33*, *44*, and references therein). To account for this contribution, we subtracted a constant fraction of 30%. This value was recently experimentally determined for the excitation conditions used in this study as outlined in ref *33*. A target fit performed with this correction for the ^{3}Car effect leads to the results shown in Figure 6 and summarized in Table 4. In perfect agreement with ref *33*, the general feature of the oscillation pattern of the normalized amplitude for the nanosecond component in the H_2O samples closely resembles that of the corresponding 830 nm absorption changes while remarkable differences between both parameters exist for the 20−40 μs kinetics. The latter phenomenon has been explained by a more complex nature of the 20−40 μs kinetics which comprises the coupling of P680$^{+\bullet}$ reduction by Y$_Z$ with additional reaction(s) as briefly outlined in ref *33* and analyzed in more detail in the present study. With respect to H/D exchange effects, an inspection of the data of Figure 6 unravels several characteristic features: (i) the pronounced oscillation of the normalized amplitude of the nanosecond kinetics of the H_2O sample almost disappears in the D_2O sample (the same phenomenon is observed for the 830 nm measurements; see Figure 2 and Table 1); (ii) except for the markedly different half-lifetimes after the first flash, the normalized amplitudes of the 2−3 and 15−30 μs kinetics are characterized by period four oscillations in both sample types; and (iii) the half-lifetimes of these two kinetics do

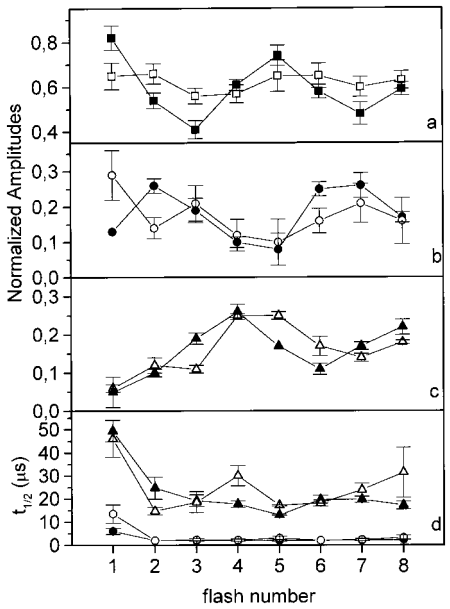

FIGURE 6: Normalized amplitudes (panels a, b, c) and half-lifetimes (panel d) of the rise components of $F(t)/F_0$ with a fixed half-lifetime of 200 ns (squares) and fast (circles) and middle (triangles) components with half-lifetimes taken as free running parameter as a function of flash number in spinach thylakoids suspended in H_2O (filled symbols) and D_2O (open circles). The data were obtained by a target fit of the traces shown in Figure 4 after correction for excitation energy transfer between different photosynthetic units and flash-induced transient carotenoid triplet population (for details, see text). The error bars indicate the spread of results over two sets of experiments with different thylakoid preparations. Error bars were omitted when both fits led to the same result.

Table 4: Target Fit with Three Exponentials and Fixed Half-Lifetime of 200 ns for the Very Fast Component[a]

flash number	A_{200ns}	A_f	$\tau_{1/2,f}$	A_m	$\tau_{1/2,s}$	A_{ss}
			pH 6.5			
1	0.82	0.13	6.1	0.05	49	0.00
2	0.54	0.26	2.1	0.10	25	0.10
3	0.41	0.19	2.1	0.19	19	0.14
4	0.61	0.10	2.1	0.26	18	0.03
5	0.74	0.08	2.1	0.17	13	0.00
6	0.58	0.25	2.1	0.11	20	0.05
7	0.48	0.26	2.1	0.17	20	0.09
8	0.59	0.17	2.5	0.22	17	0.02
			pD 6.5			
1	0.65	0.29	13.6	0.06	46	0.00
2	0.66	0.14	2.1	0.12	15	0.07
3	0.56	0.21	2.4	0.11	19	0.12
4	0.57	0.12	2.3	0.25	30	0.05
5	0.65	0.10	3.1	0.25	17	0.00
6	0.65	0.16	2.1	0.17	18	0.01
7	0.60	0.21	2.4	0.14	24	0.05
8	0.63	0.16	3.3	0.18	31	0.03

[a] The data were additionally corrected for ^{3}Car triplets as described in the text.

not exhibit a pronounced kinetic H/D exchange effect in all flashes but only after flashes no. 1, 4, 5, and 8.

A very important implication of the results presented in this study is the significant enhancement of the extent of $P680^{+\bullet}Q_A^{-\bullet}$ recombination due to replacement of exchangeable protons by deuterons. On the basis of the target fit presented in Figure 2 and Table 1, the averaged normalized extent of the 150 μs kinetics increases from 7.5% to about 20%. This feature and the oscillation pattern can be explained by a higher population probability of Y_Z^{OX} which depends on the redox state S_i of the WOC. In addition, the recombination reaction described by rate constant $k(Q_A^{-\bullet})$ competes with the $P680^{+\bullet}$ reduction by Y_Z symbolized by rate constant $k(Y_Z)$. For the sake of simplicity the possibility of electron donation by additional components (Chl, Car) will be ignored because this does not affect the general conclusions [only the quantitative values of $k(Q_A^{-\bullet})$ and $k(Y_Z)$ would be modified]. The fraction of the former process is given by $k(Q_A^{-\bullet})/[k(Q_A^{-\bullet}) + k(Y_Z)]$. In the more likely case of a significant retardation on the 35 μs kinetics due to H/D isotope exchange (vide supra), the relation $k(Q_A^{-\bullet})/[k(Q_A^{-\bullet}) + k(Y_Z)]$ leads with the results of the target fit data shown in Figure 3 and Table 2 to the following values: $k(Y_Z) = (80\ \mu s)^{-1}$ and $(285\ \mu s)^{-1}$ for the H_2O sample and D_2O sample, respectively, and contributions of the back reaction of about 3% and 9%, respectively. If one adds the constant fractions of 6% and 9% used for the target fit, the contribution of the back reaction calculates to 9% and 18% of the total extent of $P680^{+\bullet}$ reduction. Although the kinetic retardation mechanism appears to be more likely (vide supra), for the sake of comparison, the above-mentioned analysis was also performed for the case of invariant rate constants $k(Y_Z)$ but H/D-dependent amplitudes. In this case of fixed values for $[k(Q_A^{-\bullet}) + k(Y_Z)] = \ln 2/t_{1/2} = (50\ \mu s)^{-1}$ and $k(Q_A^{-\bullet}) = (215\ \mu s)^{-1}$ the back reaction contributes about 23% to the normalized extent of the 35 μs kinetics, that is, 3% of the total $P680^{+\bullet}$ reduction. Taking into account the normalized amplitudes of the 150 μs kinetics, the extent of the back reaction is expected to be about 10% in the H_2O sample and 23% in the D_2O sample.

The analysis clearly shows that, regardless of the underlying mechanism, the results of this study lead to a consistent picture; that is, the extent of the $P680^{+\bullet}Q_A^{-\bullet}$ recombination reaction increases when exchangeable protons are replaced by deuterons. The increase is calculated to be about 10% of the total $P680^{+\bullet}$ reduction kinetics. This conclusion has two important consequences: (i) the total amplitude of the normalized flash-induced changes of the fluorescence yield is expected to decrease by 15−20% in the D_2O sample compared with that of the H_2O sample when taking into account the nonlinear relationship between fluorescence yield and quencher concentration; and (ii) the probability of misses in the period four oscillation pattern of flash-induced oxygen evolution is expected to increase significantly due to H/D exchange. A comparison of the traces in Figure 4 (top and middle panel) indicates that the average value of the total $F(100\ \mu s)/F_0$ drops down by 17% when thylakoids are suspended in D_2O instead of H_2O buffer. This value in in perfect agreement with the expectation. Likewise, measurements of the oxygen yield induced by a train of saturating flashes reveal that, in thylakoids at pH = 6.5, the probability of misses increases from 7.5% to about 12% after suspension in D_2O (*64*).

Both of these findings highly support the above-mentioned conclusion of an increased $P680^{+\bullet}Q_A^{-\bullet}$ recombination due to replacement of exchangeable protons by deuterons.

DISCUSSION

The present study confirms that, in contrast to previous reports (*28*, *29*), the 2−4 and 20−40 μs kinetics of $P680^{+\bullet}$ reduction by Y_Z reflect reactions of PS II complexes with

an intact WOC. They exhibit a pronounced period four oscillation that becomes significantly modified when exchangeable protons are replaced by deuterons. A detailed analysis of 830 nm absorption changes and the rise of the normalized fluorescence quantum yield induced by a train of eight saturating flashes in dark-adapted PS II membrane fragments and thylakoids lead to the following conclusions: (a) the fraction of the microsecond kinetics in the $P680^+$ reduction kinetics under almost equilibrated S_i state population of the WOC (average of eight flashes) is only slightly affected by H/D exchange, in perfect correspondence with the results reported in ref *38*; (b) in D_2O samples the contribution of the $P680^{+\bullet}Q_A^{-\bullet}$ recombination to the total $P680^{+\bullet}$ reduction markedly increases most likely due to a comparatively large kinetic H/D isotope exchange effect on the 35 μs kinetics; and (c) the effects strongly depend on the redox state S_i of the WOC, the fast kinetics are most affected in S_0 and S_1 (first, fourth, fifth, and eighth flashes) and weakly in S_2 and S_3 (second, third, sixth, and seventh flashes) whereas the opposite is observed for the slow kinetics, that is, pronounced effects in S_2 and S_3.

On the basis of these findings questions arise on the origin of the S_i state-dependent microsecond kinetics and their modulation through replacement of exchangeable protons by deuterons. It has recently been discussed that the microsecond kinetics reflect relaxation(s) in the environment of Y_Z^{OX} coupled with proton rearrangement(s) (*32*, *33*). This gives rise to a further decrease of the population probability of $P680^{+\bullet}$. The present study highly supports this idea. Accordingly, the reduction of $P680^{+\bullet}$ by Y_Z can be described in the most simple case by the following scheme:

$$P680^{+\bullet}Y_Z \rightarrow (P680^{+\bullet}\, Y_Z \rightleftharpoons P680\, Y_Z^{OX})_{initial} \rightarrow (P680^{+\bullet}\, Y_Z \rightleftharpoons P680\, Y_Z^{OX})_{relaxed} \quad (1)$$

In agreement with a proposal in ref *32*, it is assumed that the first step occurs in the nanosecond time domain and the second symbolizes the overall relaxation process which takes place in the microsecond time domain. The percentage of total $P680^{+\bullet}$ reduction is higher in the relaxed state $((P680^{+\bullet}Q_A^{-\bullet} \rightleftharpoons P680Y_Z^{OX})_{relaxed}$ than in the intial state $(P680^{+\bullet}Q_A^{-\bullet} \rightleftharpoons P680Y_Z^{OX})_{initial}$.

We have previously proposed that the oxidation of Y_Z by P680 is coupled with a proton shift to a nearby acceptor group, by a reaction of the type (*8*):

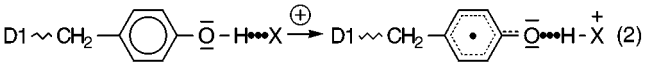

(2)

where X represents an amino acid residue and D1 the polypeptide D1. The reaction of type (2) was proposed to explain the weak temperature dependence of $P680^{+\bullet}$ reduction in the nanosecond time domain (*8*). This implies that the mode of hydrogen bonding between Y_Z and X is essential for the electron transfer via nanosecond kinetics. The strength of this bond also determines the tyrosinate anion character of Y_Z in its reduced form via the population probability of state

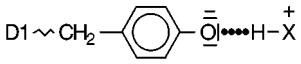

The idea of tyrosinate which has been originally proposed and discussed in ref *55* is in perfect agreement with the above-mentioned mechanism. It is assumed that strength and geometry of hydrogen bonding determine the population probability of $P680Y_Z^{OX}$ within the initial state $(P680^{+\bullet}Y_Z \rightleftharpoons P680Y_Z^{OX})_{initial}$.

With respect to the nature of group X, modeling studies (*56*, *57*) suggest that it is likely to be His 190 of polypeptide D1. This assignment is highly supported by studies of mutants where His 190 is replaced by Phe or Tyr (*58*−*60*) and Glu or Asp (*61*, *62*). It has been concluded that changes of the interaction with Y_Z give rise to a significant shift of the equilibrium $P680^{+\bullet}Y_Z \rightleftharpoons P680Y_Z^{OX}$ toward the left side (*60*). A similar effect has been discussed for the mutant H195D of polypeptide D1 (*59*). A recent detailed study on the kinetics of $P680^{+\bullet}$ reduction, Y_Z oxidation (Y_Z^{OX} reduction), and $Q_A^{-\bullet}$ reoxidation in PS II particles from mutants of *Synechocystis sp.* PCC 6803, where His 190 is replaced by eight different amino acids, provides convincing evidence for the assignment of group X to His 190 of polypeptide D1 (*63*). The idea of a strong hydrogen bonding of Y_Z^{OX} is supported by recent FTIR data (*65*).

The model summarized by eq 1 implies that the extent of $P680^{+\bullet}Q_A^{-\bullet}$ reduction increases due to the relaxation reaction(s) in the microsecond time domain. If these reactions are retarded, the state $(P680^{+\bullet}Y_Z)_{initial}$ is kinetically "arrested" in a fraction of PS II for a longer time. In this case the recombination reaction of $P680^{+\bullet}$ with $Q_A^{-\bullet}$ which is characterized by a 150 μs half-lifetime (*25*, *26*) efficiently competes with electron donation from Y_Z.

Accordingly, the pronounced H/D isotope exchange effect can be explained by the assumption that the relaxation reaction(s) is(are) dominated via rearrangement of a hydrogen bond network. The replacement of exchangeable protons by deuterons is inferred to retard the relaxation process(es), and therefore the percentage of back reaction increases. Since $P680^{+\bullet}Q_A^{-\bullet}$ recombination is dissipative for the S_i state transitions in the WOC, the probability of misses has to increase when exchangeable protons are replaced by deuterons. Recent measurements of the oscillation pattern of the oxygen yield induced by a flash train in dark-adapted H_2O samples and D_2O samples showed this to be the case. Ratios of about 1.6 were found for $\alpha(D)/\alpha(H)$ at pL = 6.5 (*64*).

A very interesting consequence of the present model is the conclusion that the nanosecond kinetics disappear when the hydrogen-bonded states

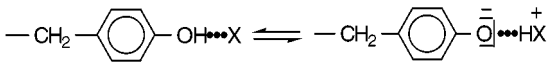

are destroyed by protonation of X. Accordingly, the normalized extent of the nanosecond kinetics is expected to decrease concomitantly with an increase of the α-values and decrease of the average oxygen yield per flash. Our previous and recent results (*64*, *66*, *67*) support this conclusion. A more detailed analysis will be presented in a forthcoming paper (Christen, G., Seeliger, A., and Renger, G., submitted to *Biochemistry*).

Independent lines of evidence for a structural tuning of $P680^{+\bullet}$ reduction by Y_Z has been previously proposed on the basis of different types of experiments (*68*−*70*). It was found that the ratio of the normalized amplitudes of

nanosecond and microsecond kinetics becomes markedly shifted toward the latter one when PS II membrane fragments are subjected to a very mild trypsin treatment that does not significantly affect the oxygen evolution capacity (*69*). This effect is dependent on light (*69*) and can be largely reversed by Ca^{2+} in a very specific manner including binding sites with two different affinity constants (*68*−*70*).

With respect to the proposed mechanism for the multiphasic $P680^{+\bullet}$ reduction by Y_Z another striking feature has to be taken into consideration. It is well-known that the kinetics of this reaction depend on the redox state S_i of the WOC (*8*, *14*, *30*). This effect has been ascribed to the electrostatic effect of a positive surplus charge in S_2 and S_3 (*14*), although alternative mechanisms such as a conformational gating cannot be excluded as discussed in ref *68*. In relation to the kinetic modulation, the present study and the recent report of Schilstra et al. (*32*) describe very interesting findings. The results obtained here clearly show that the H/D isotope exchange effect on the fast kinetics is most pronounced when the WOC attains the redox states S_0 and/or S_1 while more pronounced changes are observed for the slow kinetics in S_2 and S_3. On the basis of the assignment to relaxation processes within a hydrogen bond network in the environment of Y_Z^{OX} the marked S_i state dependence of the H/D exchange effect on the fast $P680^{+\bullet}$ reduction kinetics is not easily reconcilable with a simple electrostatic effect caused by a single localized charge. It might rather reflect, at least in part, structural differences of the WOC in redox states S_0, S_1 versus S_2, S_3. This raises questions on the mode of "communication" between Y_Z and the WOC. At a first glance, the most simple idea is a close interaction via a comparatively short distance between Y_Z and the manganese cluster of about 3.5 Å (*71*). However, it has to be emphasized that a hydrogen bond network can be rather extended so that the effect of the redox state S_i of the relaxation processes is also in line with the markedly longer distances reported in the literature (*24*, *39*, *72*−*74*). The physiological relevance of this mode of S_i state-dependent regulation has to be clarified in future studies.

ACKNOWLEDGMENT

The authors would like to thank Dr. F. Reifarth for his invaluable contributions in development of equipment and programming.

NOTE ADDED IN PROOF

The very short distance between Y_Z and the manganese cluster noted in the paragraph above (3.5 Å) has been shown to originate from incorrect data interpretation and therefore to be enlarged to 9−12 Å (*75*).

REFERENCES

1. Debus, R. J. (1992) *Biochim. Biophys. Acta 1102*, 269−352.
2. Renger, G. (1993) *Photosynth. Res. 38*, 229−247.
3. Haumann, M., and Junge, W. (1996) in *Oxygenic Photosynthesis: The Light Reactions* (Ort, D. R., and Yocum, C. F., Eds.) pp 165−192, Kluwer Academic Press, Dordrecht, The Netherlands.
4. Renger, G. (1992) in *Topics in Photosynthesis, The Photosystems: Structure, Function and Molecular Biology* (Barber, J., Ed.) pp 45−99, Elsevier, Amsterdam, The Netherlands.
5. Debus, R. J., Barry, B. A., Sithole, I., Babcock, G. T., and McIntosh, L. (1988) *Biochemistry 27*, 9071−9074.
6. Metz, J. G., Nixon, P. J., Rögner, M., Brudvig, G. W., and Diner, B. A. (1989) *Biochemistry 28*, 6960−6969.
7. Babcock, G. T., Barry, B. A., Debus, R. J., Hoganson, C. W., Atamian, M., McIntosh, L., Sithole, U., and Yocum, C. G. (1989) *Biochemistry 28*, 9557−9565.
8. Eckert, H.-J., and Renger, G. (1988) *FEBS Lett. 236*, 425−431.
9. Tommos, C., and Babcock, G. T. (1998) *Acc. Chem. Res. 31*, 18−25.
10. Babcock, G. T. (1995) in *Photosynthesis: from light to biosphere* (P. Mathis, Ed.) Vol. II, pp 209−215, Kluwer Academic Publishers, Dordrecht, The Netherlands.
11. Renger, G. (1997) *Physiol. Plant. 100*, 828−841.
12. Renger, G. (1997) in *Treatise on Bioelectrochemistry* Gräber, P., and Milazzo, G., Eds.) Vol. 2: Bioenergetics, pp 310−358, Birkhäuser Verlag, Basel, Germany.
13. Renger, G., Eckert, H.-J., and Weiss, W. (1983) in *The oxygen evolving system in photosynthesis* Inoue, Y., Crofts, A. R., Govindjee, Murata, N., Renger, G., and Satoh, K., Eds.) pp 73−82, Academic Press, Japan.
14. Brettel, K., Schlodder, E., and Witt, H. T. (1984) *Biochim. Biophys. Acta 766*, 403−415.
15. Eckert, H.-J., Renger, G., and Witt, H. T. (1984) *FEBS Lett. 167*, 316−320.
16. Eckert, H.-J., Wydrzynski, T., and Renger, G. (1988) *Biochim. Biophys. Acta 932*, 240−249.
17. Yamashita, T., and Butler, W. L. (1968) *Plant Physiol. 43*, 1978−1986.
18. Cheniae, G. M., and Martin, I. F. (1971) *Plant Physiol. 47*, 568−575.
19. Conjeaud, H., and Mathis, P. (1980) *Biochim. Biophys. Acta 590*, 353−359.
20. Renger, G., Völker, M., and Weiss, W. (1984) *Biochim. Biophys. Acta 766*, 582−591.
21. Weiss, W., and Renger, G. (1986) *Biochim. Biophys. Acta 850*, 173−183.
22. Reinman, S., and Mathis, P. (1981) *Biochim. Biophys. Acta 635*, 249−258.
23. Ahlbrink, R., Haumann, M., Cherepanov, D., Bögershausen, O., Mulkidjanian, A., and Junge, W. (1998) *Biochemistry 37*, 1131−1142.
24. Renger, G., Christen, G., Karge, M., Eckert, H.-J., and Irrgang, K.-D. (1998) *J. Biol. Inorg. Chem. 3*, 360−366.
25. Renger, G., and Wolff, Ch. (1976) *Biochim. Biophys. Acts 423*, 610−614.
26. Haveman, J., and Mathis, P. (1976) *Biochim. Biophys. Acta 440*, 346−355.
27. Renger, G. (1979) *Biochim. Biophys. Acta 547*, 103−116.
28. Hoganson, C. W., Casey, P. A., and Hansson, Ö. (1991) *Biochim. Biophys. Acta 1057*, 399−406.
29. Schlodder, E., Brettel, K., and Witt, H. T. (1985) *Biochim. Biophys. Acta 808*, 123−131.
30. Gläser, M., Wolff, Ch., and Renger, G. (1976) *Z. Naturforsch., C: Biosci. 31*, 712−721.
31. Lukins, P. B., Post, A., Walker, P. J., and Larkum, A. W. D. (1996) *Photosynth. Res. 49*, 209−221.
32. Schilstra, M. J., Rappaport, F., Nugent, J. H. A., Barnett, C. J., and Klug, D. R. (1998) *Biochemistry 37*, 3974−3981.
33. Christen, G., Reifarth, F., and Renger, G. (1998) *FEBS Lett. 429*, 49−52.
34. Renger, G., Eckert, H.-J., and Buchwald, H.-E. (1978) *FEBS Lett. 90*, 10−14.
35. Eckert, H. J., and Renger, G. (1980) *Photochem. Photobiol. 31*, 501−511.
36. Mathis, P., and Rutherford, A. W. (1984) *Biochim. Biophys. Acta 767*, 217−222.
37. Thompson, K. L., Miller, A. F., De Paula, J. C., and Brudvig, G. W. (1988) *Isr. J. Chem. 28*, 121−128.
38. Karge, M., Irrgang, K.-D., Sellin, S., Feinäugle, R., Liu, B., Eckert, H.-H., Eichler, H. J., and Renger, G. (1996) *FEBS Lett. 378*, 140−144.

39. Karge, M., Irrgang, K.-D., and Renger, G. (1997) *Biochemistry 36*, 8904−8913.
40. Christen, G., Karge, M., Eckert, H.-J., and Renger, G. (1997) *Photosynthetica 33*, 529−539.
41. Winget, G. D., Izawa, S., and Good, N. E. (1965) *Biochem. Biophys. Res. Commun. 21*, 438−443R.
42. Berthold D. A., Babcock G. T., and Yocum, C. A. (1981) *FEBS Lett. 134*, 231−234.
43. Völker, M., Ono, T., Inoue, Y., and Renger, G. (1985) *Biochim. Biophys. Acta 806*, 25−34.
44. Reifarth, F., Christen, G., and Renger, G. (1997) *Photosynth. Res. 51*, 231−242.
45. Glasoe, P. K., and Long. F. A. (1969) *J. Phys. Chem. 64*, 188−190.
46. Ostermeier, A. (1992) in *Proceedings of the 2nd Conference on parallel problems soving from nature* (Männer, R., and Manderick, B., Eds.) pp 197−206, Elsevier, Amsterdam, The Netherlands.
47. Joliot, P., and Joliot, A. (1964) *C. R. Acad. Sci. Paris 258*, 4622−4625.
48. Dohnt, G., and Renger, G. (1984) in *Advances in Photosynthesis Research*, (Sybesma, C., Ed.) Vol. 1 pp 429−432, Martinus Nijhoff/Dr. W. Junk Publishers, Den Haag, The Netherlands.
49. Renger, G., Eckert, H.-H., Hagemann, R., Hanssum, B., Koike, H., and Wacker, U. (1989) in *Photosynthesis: Molecular Biology and Bioenergetics* (Singhal, G. S., Barber, J., Dilley, R. A., Govindjee, Haselkorn, R., and Mohanty, P., Eds.) pp 357−371, Narosa Publishing House, New Delhi, India.
50. Renger, G., Bittner, T., and Messinger, J. (1994) *Biochem. Soc. Trans. 22*, 318−322.
51. Butler, W. L. (1972) *Proc. Natl. Acad. Sci. U.S.A. 69*, 3420−3422.
52. Joliot, P., and Joliot, A. (1972) in *Photosynthesis, two centuries after its discovery by Joseph Priestly* (Forti, G., Avron, M., and Melandri A., Eds.) Vol. 1, pp 26−38, Dr. W. Junk Publishers, The Hague, The Netherlands.
53. Delosme, R. (1972) in *Photosynthesis, two centuries after its discovery by Joseph Priestly* (Forti, G., Avron, M., and Melandri, A. Eds.) Vol. 1, pp 187−195, Dr. W. Junk Publishers, The Hague, The Netherlands.
54. Schödel, R., Irrgang, K. D., Voigt, J., and Renger, G. (1998) *Biophys. J. 75*, 3143−3153.
55. Candeias, L. P., Turconi, S., and Nugent, J. H. A. (1998) *Biochim. Biophys. Acta 1363*, 1−5.
56. Ruffle, S. V., Donelly, D., Blundell, T. L., and Nugent, J. H. A. (1992) *Photosynth. Res. 34*, 287−300.
57. Svensson, B., Etchebest, C., Tuffery, P., van Kan, P., Smith, J., and Styring, S. (1996) *Biochemistry 35*, 14486−14502.
58. Kullander, C., Fredriksson, P.-O., Sayre, R. T., Minagowa, J., Crofts, A. R., and Styring, S. (1995) in *Photosynthesis: from light to biosphere* (Mathis, P., Ed.) Vol. II pp 321−324, Kluwer Academic Publishers, Dordrecht, The Netherlands.
59. Roffey, R. A., Kramer, D. M., Govindjee, and Sayre, R. T. (1994) *Biochim. Biophys. Acta 1185*, 257−270.
60. Roffey, R. A., van Wijk, K. J., Sayre, R. T., and Styring, S. (1994) *J. Biol. Chem. 269*, 5115−5121.
61. Diner, B. A., Nixon, P. J., and Forchaus, J. W. (1991) *Curr. Opin. Struct. Biol. 1*, 546−554.
62. Nixon, P. J., and Diner, B. A. (1992) *Biochemistry 31*, 942−948.
63. Hays, A.-M. A., Vassiliev, I. R., Golbeck, J. H., and Debus, R. J. (1998) *Biochemistry 37*, 11352−11365.
64. Renger, G., Christen, G., and Seeliger, A. (1998) in *Proceedings XI International Photosynthesis Congress* (in press).
65. Berthomieu, C., Hienerwadel, R., Boussac, A., Breton, J., and Diner, B. A. (1998) *Biochemistry 37*, 10547−10554.
66. Renger, G., Gläser, M., and Buchwald, H.-E. (1977) *Biochim. Biophys. Acta 461*, 392−402.
67. Messinger, J., and Renger, G. (1994) *Biochemistry 33*, 10896−10905.
68. Renger, G., Eckert, H.-J., and Völker, M. (1989) *Photosynth. Res. 22*, 247−256.
69. Völker, M., Eckert, H.-J., and Renger, G. (1987) *Biochim. Biophys. Acta 890*, 66−77.
70. Völker, M., Eckert, H.-J., and Renger, G. (1987) in *Prog. Photosynth. Res.* (Biggins, J., Ed.) Vol. 1, pp 545−548, Martinus Nijhoff/Dr. W. Junk Publishers, Dordrecht, The Netherlands.
71. Force, D. A., Randall, D. W., and Britt, R. D. (1997) *Biochemistry 36*, 12062−12070.
72. Astashkin, A. V., Mino, H., Kawamori, A., and Ono, T. (1997) *Chem. Phys. Lett. 272*, 506−516.
73. Mulkidjanian, A., Cherepanov, D. A., Haumann, M., and Junge, W. (1996) *Biochemistry 35*, 3093−3107.
74. Un, S., Brunel, L.-C., Brill, T. M., Zimmermann, J.-L., and Rutherford, A. W. (1994) *Proc. Natl. Acad. Sci. U.S.A. 91*, 5262−5266.
75. Peloquin, J. M., Campbell, K. A., and Britt, R. D. (1998) *J. Am. Chem. Soc. 120*, 6840−6841.

BI982188T